Hopping conductivity and ac magnetoresistance of p-type InSb using acoustic measurements

F. Guillon,* B. Fernandez,† G. Madore,‡ and J. D. N. Cheeke
Centre de Recherche en Physique du Solide et Département de Physique, Université de Sherbrooke, Sherbrooke, Québec, Canada J1K 2R1
(Received 31 May 1988; revised manuscript received 19 April 1989)

The conductivity and magnetoresistance of lightly doped p-type InSb in the hopping regime have been studied between 0.1 and 20 K by ultrasonic attenuation measurements. The conductivity in zero magnetic field has been obtained through the analysis of attenuation data with the Hutson-White model for piezoelectric semiconductors. The data are consistent with the simple theory without the diffusion term. Magnetoacoustic data for the sample with the lowest concentration (10^{14} cm^{-3}) has shown frequency-dependent negative magnetoresistance at low field ($H<20$ kG) and a strong frequency-dependent positive magnetoresistance at a higher field. This frequency-dependent positive magnetoresistance has been explained within the framework of the scaling theory of Summerfield for the ac conductivity of disordered solids.

I. INTRODUCTION

The transport properties of group III-V semiconductors have been extensively studied at low temperatures. Surface conduction in contaminated layers is recognized as a major difficulty which can greatly affect measurements of the electrical conductivity and the Hall effect at low temperatures[1] in the regime where electrons freeze-out from the conduction band. The piezoelectric interaction in some semiconductors has permitted the study of the electrical properties by acoustic measurements. Extensive measurements[2,3] of attenuation and velocity shift in p-type InSb have clearly demonstrated the potential of acoustic methods to characterize the conductivity regime in this doped semiconductor, where conductivity is thermally activated with an ionization energy ε_1. The present paper deals with the study of the conductivity in p-type InSb by acoustic measurements methods in the regime where thermal freeze-out occurs. In this regime, conductivity is by a hopping process. Our previous work[4] has clearly shown the occurrence of the frequency-dependent ac conductivity in this regime.

In this paper, we report on the temperature dependence of the acoustic attenuation and on the ac magnetoresistance derived from the magnetic-field dependence of the acoustic attenuation in p-type InSb in the hopping regime. Under some conditions which will be discussed, negative magnetoresistance was observed for the first time by acoustic measurements.

II. BACKGROUND THEORY

In piezoelectric semiconductors, numerous experiments[2,5,6] have demonstrated that the Hutson and White model[7] well described the acoustic attenuation due to the electrons. Previous studies in p-type InSb in the thermally activated regime have shown that diffusion effect can be neglected. The sound attenuation is then given by

$$\alpha=\frac{K^2\omega}{2V_{so}}\frac{\omega_c/\omega}{1+(\omega_c/\omega)^2}\ , \tag{1}$$

where K^2 is the electromechanical coupling coefficient, V_{so} the sound velocity, and $\omega_c=\sigma/\varepsilon$ the relaxation frequency. Figure 1 shows a plot of Eq. (1) as a function of the conductivity for the piezoelectric longitudinal mode in InSb. At any given frequency, the attenuation goes through a relaxation peak as the conductivity is varied. Measurements[2] have confirmed that the acoustic attenuation passes through a maximum near 10 K in the activated regime where the conductivity σ is such that $\omega_c=\omega$. Alternatively, we can use Eq. (1) to study the behavior of the electrical conductivity by measuring the change in the acoustic attenuation as a function of temperature or magnetic field. The results that will be presented in this paper lie in the hopping regime where the conductivity is low compared to the value observed at the relaxation peak. In this regime, $\omega_c \ll \omega$, the attenuation is directly

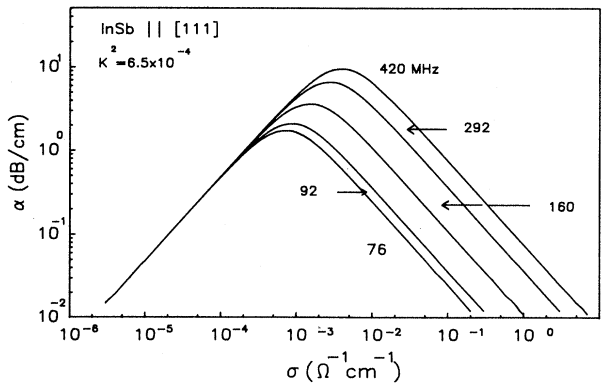

FIG. 1. Acoustic attenuation in InSb according to the Hutson-White model, Eq. (1). The curves show a maximum at a specific conductivity.

proportional to the conductivity

$$\alpha = \frac{K^2 \sigma}{2 V_{so} \varepsilon} . \quad (2)$$

III. EXPERIMENTAL METHODS

For the measurements we used single crystals of p-type InSb obtained from Cominco Ltd. The samples were compensated with excess concentrations of Ge of 10^{14}, 3.4×10^{14}, and 7.5×10^{15} cm^{-3}. Except where indicated, all acoustic measurements were done with the longitudinal piezoelectric mode along [111]. For experiments above 2 K we used a double calorimeter cryostat in conjunction with a 70 kG magnet. The temperature was measured by silicon diode and capacitance thermometer. For measurements at lower temperatures ($0.1 < T < 4.2$ K), a dilution refrigerator of standard design was used with a 50 kG magnet. Calibrated germanium sensors and a Speer resistor were used for temperature measurements.

To avoid problems with acoustic bonds for the experiments performed with the dilution refrigerator, ZnO transducers[8] were used on the InSb samples. For the experiments with the double calorimeter, $LiNbO_3$ transducers bonded with silicone oil and ZnO transducers were both used. Using the known behavior of the relaxation peak near 10 K in zero magnetic field we checked that, within the experimental errors, the measurements obtained with both type of transducers were equivalent.

Pulsed acoustic attenuation measurements were performed using standard equipment. At very low temperatures, the lowest acoustic power which gave a reasonable signal-to-noise ratio, was used. There was no indication of sample heating at this power level. Sample mountings were made with standard methods and are described in detail elsewhere.[9-11]

IV. RESULTS AND DISCUSSION

A. Acoustic attenuation in $H=0$

The results of the attenuation at low temperatures in zero magnetic field are shown in Fig. 2 for the three concentrations used in the present study. Similar data are shown in Fig. 3 but for temperatures well below 4.2 K. In a previous study,[2,10] it was noticed that systematically the attenuation at 4.2 K (the minimum temperature in these experiments) was always slightly higher than the attenuation near 20 K. This attenuation difference was more noticeable at higher frequencies. Separate experiments[10] on the nonpiezoelectric mode had indicated negligible phonon attenuation below 20 K and that this attenuation was probably residual at this temperature. Consequently the existence of an extra attenuation at 4.2 K above this residual attenuation raises the question as to whether it is a new attenuation mechanism for piezoelectric modes at 4.2 K. These considerations motivated us to extend the previous work to lower temperatures to elucidate the nature of the extra attenuation. The results in Fig. 3 show that there is indeed a drop in the measured attenuation, in particular below about 2.5 K. Furthermore, we can see that at least for the sample 3 (Fig. 2), the attenuation at the lowest temperatures tends towards the constant high-temperature residual attenuation. For the two other samples it was not possible to measure the variation of the attenuation over such a large temperature range in a single run.

For a sufficient sensitivity in attenuation measurements the smaller change below 2 K required the use of two

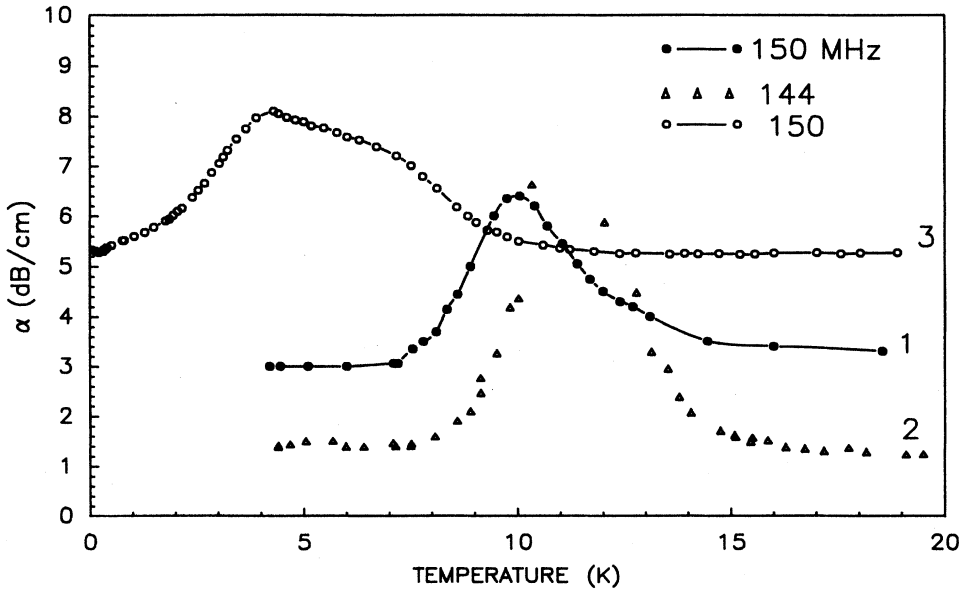

FIG. 2. Acoustic attenuation along [111] vs temperature. Numbers 1,2,3 refer to excess concentrations of 10^{14}, 3.4×10^{14}, and 7.5×10^{15} cm^{-3}, respectively.

echoes widely separated in time. With these same echoes, however, it was not generally possible to measure the full relaxation peak at higher temperature with the dynamic range of about 30 dB for our ultrasonic equipment. Therefore, attenuation measurements for the two other samples were done in two separate runs to cover the 0.1–20 K temperature range with a different selection of echoes.

These attenuation measurements at high and low temperatures have been analyzed using relation (1). At moderately low temperatures it is generally accepted that the dc electrical conductivity of doped semiconductors[12] is well represented by

$$\sigma=\sigma_1 e^{-\varepsilon_1/kT}+\sigma_2 e^{-\varepsilon_2/kT}+\sigma_3 e^{-\varepsilon_3/kT} . \quad (3)$$

Energy ε_1 represents an activation energy due to carriers excited in the valence band from acceptor impurity centers in our p-type samples. The energy ε_3 is associated with activated impurity hopping between acceptor centers at low temperatures. The second term characterized by the energy ε_2 is generally observed only for a restricted range of concentration and compensation.

The extensive work of Madore and Cheeke[2] has shown that the first and third term dominate the dc conductivity of low-density (10^{14}–10^{15} cm^{-3}) p-type InSb samples in various magnetic fields. For $T>7$ K, the acoustic attenuation is well described by the Hutson-White formula with the first term in Eq. (3) being the conductivity at high frequencies. In this regime, the conductivity is activated and independent of frequency. Figure 4 corresponds to such fit in this regime where the emphasis is put on the relaxation peak. For $T<7$ K our previous acoustic measurements showed[3,4] that the third term in the dc conductivity equation cannot be used to describe the results. Instead a frequency-dependent ac conductivity of the form $\omega^s T^n$ was invoked. At 4.2 K, frequency dependent conductivities derived from acoustic measurements gave a value of $s\sim 0.8$. In Fig. 4(b), the poor fit at the peak and at high temperature is misleading since the asymmetric peak was reproducible and is suspected to be the result of inhomogeneities in the concentration. In Fig. 4, these fits cannot distinguish at the lowest temperatures between contribution of the form $\sigma_3 e^{-\varepsilon_3/kT}$ and $\omega^s T^n$ because of the restricted range of temperature. In Fig. 5, the data for the sample with a concentration of 3.4×10^{14} cm^{-3} were plotted in an attempt to define the correct temperature dependence in the hopping regime. Below $T<4.2$ K, Eq. (2) and the frequency-dependent conductivity term $\omega^s T^n$ should give rise to a linear relationship between $\log_{10}\alpha$ and $\log_{10}T$. For this linear relationship α must be the attenuation corrected for the residual attenuation. Despite the scattering the data in Fig. 5 confirm this relationship although this figure presents the raw data including an unknown residual attenuation. On the other hand the same data could be fitted but not as well to an activated-type term as in (3) provided we use the attenuation relative to the lowest temperature $\Delta\alpha(T)=\alpha(T)-\alpha(0.1\text{ K})$. In Fig. 6 we present data at various frequencies for the sample with the lowest excess concentration. It can be seen as pointed out above that the relative attenuation can be fitted with an activated type equation. The raw data (total attenuation α) can also be fitted (not shown) to the power law T^n. Recent direct measurements of the electrical conductivity of insulating Si:P under similar conditions of frequency and temperature by Migliuolo and Castner[14] show that various laws including the power law could be used in interpreting the temperature dependence of the conductivity. The present results in the hopping regime seemed to confirm their observations. The uncertainty about the

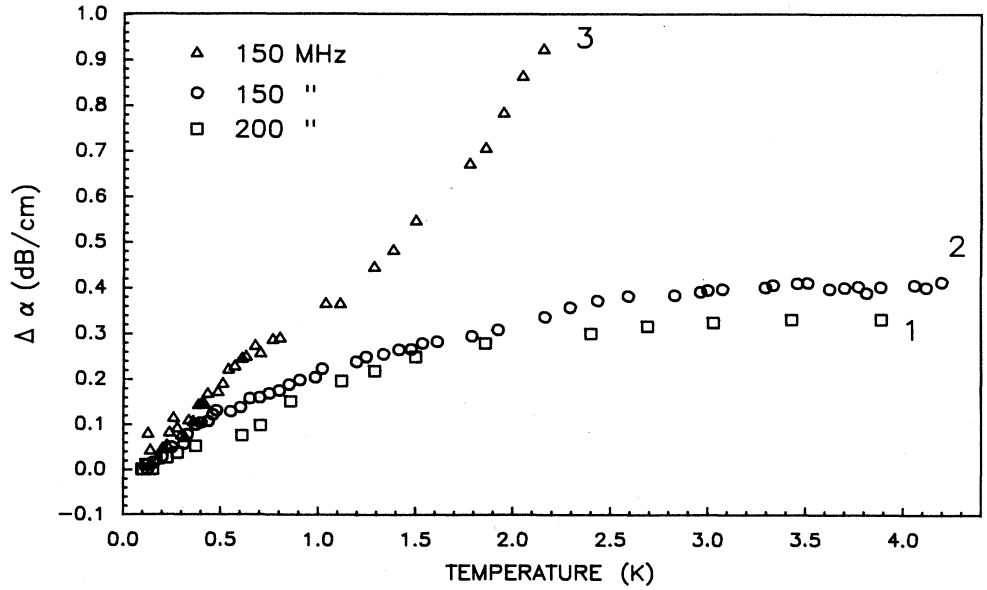

FIG. 3. Acoustic attenuation relative to 0.1 K vs temperature. Numbers 1,2,3 refer to excess concentration of 10^{14}, 3.4×10^{14}, and 7.5×10^{15} cm^{-3}, respectively.

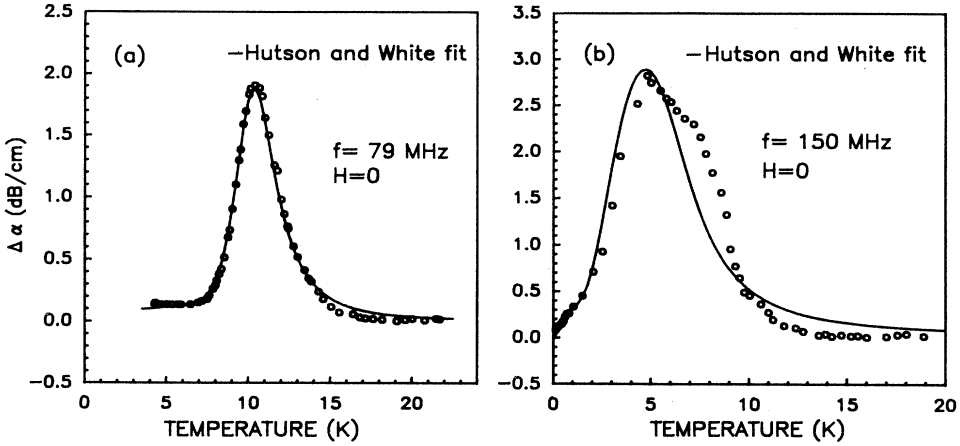

FIG. 4. Acoustic attenuation along [111] vs temperature. In (a) and (b) the solid curve represents the fit calculated with Eq. (1) for the data on sample of excess concentration 3.4×10^{14} and 7.5×10^{15} cm^{-3}, respectively. The residual attenuation was subtracted from the raw data. From these fits we deduced for ε_1 the values of 8.9 ± 0.5 and 3.49 ± 0.08 meV, respectively, for each curve in (a) and (b). These values are consistent with published values based on dc measurements (Refs. 9 and 13). Values of 0.20 and 0.77 meV can also be deduced for ε_3, but as discussed in the text, they may be meaningless.

proper law to describe the results emphasizes the need for an accurate knowledge of the residual attenuation measured in the $T=0$ limit and compared with the high-temperature limit α ($T>20$ K). The apparatus used in our experiments were not designed in view of such a wide temperature range for the measurements. Finally a wide temperature range is also essential in order to discriminate between the various laws.

B. Acoustic attenuation in the magnetic field

1. *Nonpiezoelectric mode*

Magnetoacoustic measurements were performed in nonpiezoelectric direction under various conditions to investigate any electronic contribution not related to the piezoelectric interaction so that the analysis for the piezoelectric mode could be made without ambiguity.

We show in Fig. 7 the magnetic-field dependence of the acoustic attenuation for various temperatures. Within the scatter, we did not measure any field variation. At the lowest temperatures the apparent oscillation in the attenuation can be largely explained by the limit of stability of our temperature control. For these measurements the temperature was controlled by regulating manually the pressure of the pumped bath. In this way, temperature stability was at best about ±0.05 K near 2 K. As seen in Fig. 3 the attenuation in zero field for the sample with the largest excess concentration (curve 3) is rapidly changing with temperature, therefore oscillations seen in Fig. 7 are not very significant. Figure 8 shows the measurements taken at various high frequencies for the sample with the lowest concentration. Despite the large scatter, we do

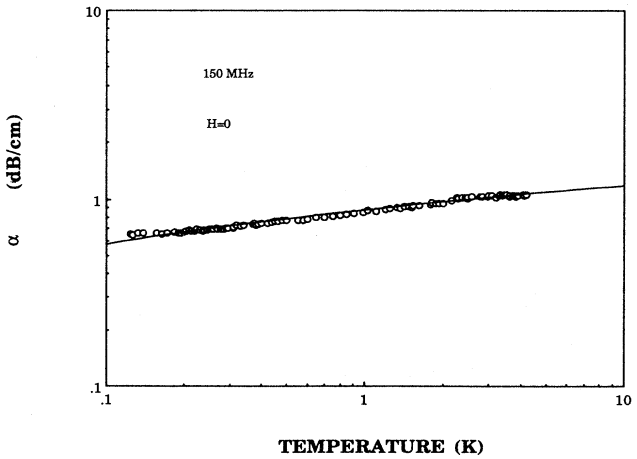

FIG. 5. Acoustic attenuation α along [111] vs temperature. The data of sample (2) in Fig. 3 are shown with a fit based on Eq. (2) and a power law $\omega^s T^n$ for the conductivity σ. A linear fit gives a value of $n=0.16$. The straight line in the figure is intended to be a guide to the eyes.

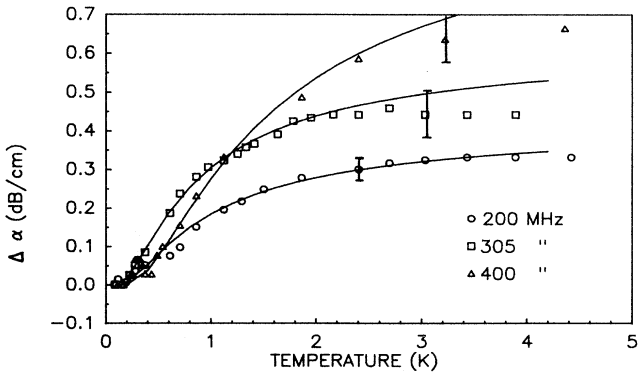

FIG. 6. Acoustic attenuation along [111] vs temperature for the sample with excess concentration of 10^{14} cm^{-3}. The solid lines represent fits based on Eq. (2) and an activated type term for the conductivity. The significance of the fits are discussed in the text.

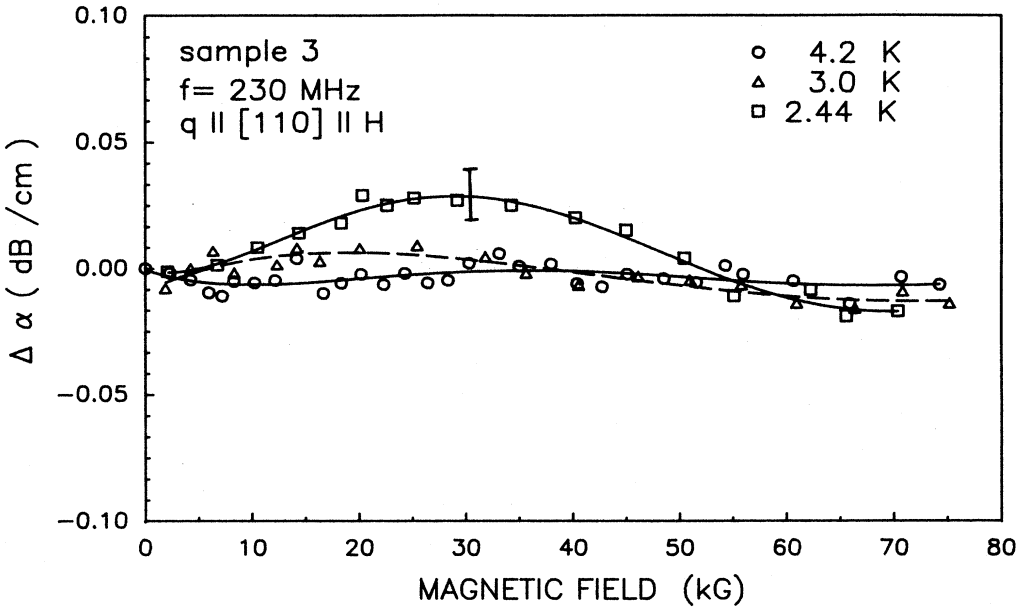

FIG. 7. Magnetic-field dependence of the acoustic attenuation along [110] for the sample with the highest excess concentration.

not see any large change, in particular, at the maximum of the magnetic field. The significance of these measurements and the solid curve will be discussed later. To summarize, no variations of the magnetoacoustic attenuation were seen either as a function of temperature or frequency.

2. *Piezoelectric mode*

The magnetic-field dependence of the acoustic attenuation for our samples with the three excess concentrations, are shown in Figs. 9–11. In all figures the same general features can be seen, namely a continuous decrease of the attenuation with higher fields at low frequency and a small maximum near 20 kG above a critical frequency.

In Fig. 8 the solid curves represent the results of Fig. 11 at the highest frequencies. It will be shown that the maximum is clearly a genuine effect due to changes in the conductivity as measured by the piezoelectric interaction. Indeed it is seen that at high field the linear extrapolation of the low-field data exceeds largely the measurements seen in the nonpiezoelectric mode. In Fig. 12 the large changes observed for the sample with the largest concentration were studied at various low temperatures.

Before analyzing in detail these experimental curves in order to obtain the electrical conductivity in a magnetic field, some features should be underlined. For all cases in zero field the temperature is low enough that the starting point corresponds to a conductivity with a value of attenuation below the attenuation peak in Fig. 1. The maximum at low field, seen in Figs. 9–12, is smaller than the relaxation peak, so it is clear that the conductivity change due to the magnetic field is not sufficient to account for the change due to the relaxation peak. Furthermore, since the attenuation is rising to a maximum, this

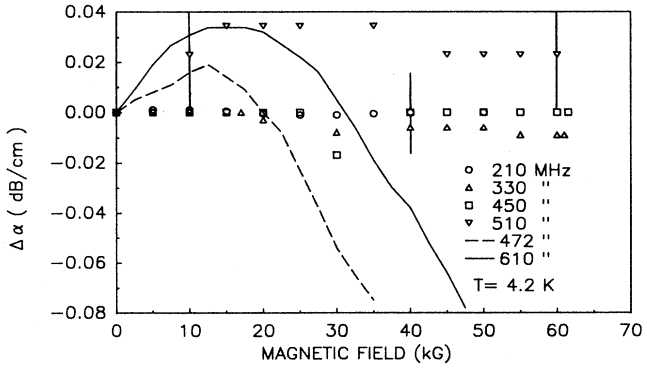

FIG. 8. Magnetic-field dependence of the acoustic attenuation for the sample with 10^{14} cm^{-3} excess concentration. The data show measurement along [110] while the solid and dashed curves represent data along [111] to be seen in Fig. 11.

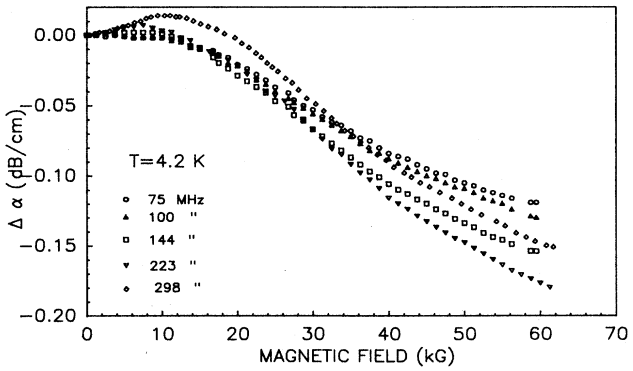

FIG. 9. Magnetic-field dependence of the acoustic attenuation at $T=4.2$ K along [111] for the sample with 3.4×10^{14} cm^{-3} excess concentration.

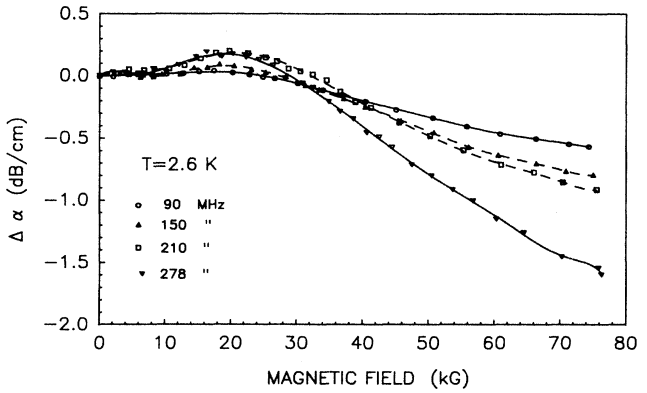

FIG. 10. Magnetic-field dependence of the acoustic attenuation at $T=2.6$ K along [111] for the sample with 7.5×10^{15} cm^{-3} excess concentration.

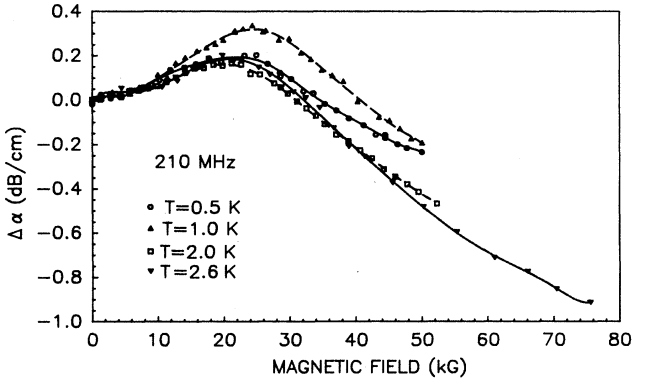

FIG. 12. Magnetic-field dependence of the acoustic attenuation along [111] for the sample with 7.5×10^{15} cm^{-3} excess concentration. These data underline the effect of temperature on the attenuation peak at low magnetic field.

small attenuation peak at low field is unambiguously associated with a rise in the conductivity. In relation to the magnetoresistance, this attenuation maximum leads us to report that we have observed negative magnetoresistance under some range of concentrations and frequencies in p-type samples. We will come back to this result later when we compared these results with our known dc magnetoresistance measurements.

The curves, depicted in Figs. 9–12, represent only the change in attenuation relative to zero field. The zero-field contribution is the sum of three terms,

$$\alpha(H=0,T)=\alpha_r(T)+\alpha_{\rm pho}(T)+\alpha_{\rm AE}(H=0,T)\ , \quad (4)$$

where the first term is the residual attenuation, the second term the phonon attenuation, and the third term is the component of interest, the acoustoelectric attenuation described by the Hutson-White model. The first and second contribution are independent of the magnetic field as we have been able to show with measurements on the nonpiezoelectric mode. The quantity of interest $\alpha_{\rm AE}(H,T)$ is related to the measured attenuation by

$$\alpha_{\rm AE}(H,T)=\alpha_{\rm AE}(0,T)+\Delta\alpha(H,T)\ . \quad (5)$$

Since we measure directly $\Delta\alpha(H,T)$, a knowledge of $\alpha_{\rm AE}(0,T)$ is sufficient to extract the quantity of interest from which we can derive the conductivity as a function of magnetic field. We have been able to obtain $\alpha_{\rm AE}(H=0,T)$ by measuring the temperature dependence of the measured attenuation in zero field. At $T>10$ K, the acoustoelectric contribution is negligible and the phonon contribution is not yet giving an observable contribution. We can then obtain the temperature-independent residual attenuation from high-temperature data.

The behavior of this residual attenuation was quite visible in Fig. 2. In Fig. 4 this residual attenuation was subtracted in fitting the data. The conductivity was then derived from the analysis of $\alpha_{\rm AE}(H,T)$ using the simplified relation for the Hutson-White model [relation (2)]. The ac conductivities derived from this procedure for our three sample concentrations are shown in Figs. 13–15. As we discussed earlier, at high frequency there is always an initial increase in the conductivity at low field, leading to a conductivity maximum. At high magnetic field there is always a continuous decrease in the electrical conductivity.

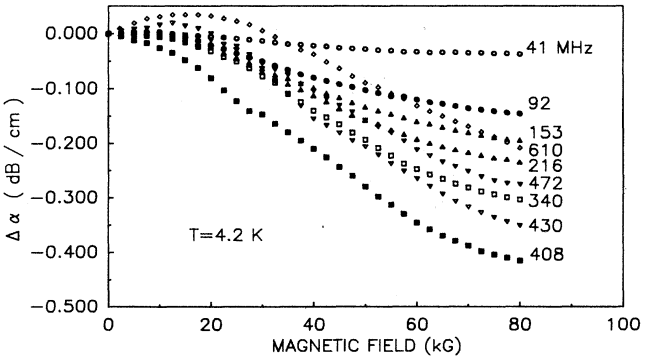

FIG. 11. Magnetic-field dependence of the acoustic attenuation along [111] at $T=4.2$ K for the sample with the lowest excess concentration (10^{14} cm^{-3}). The data emphasize the effect of frequency in the hopping regime.

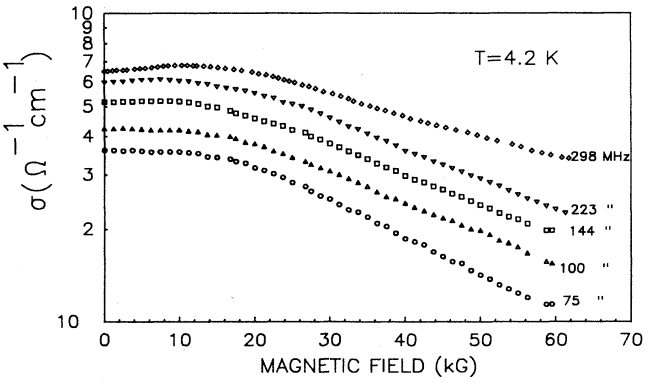

FIG. 13. ac magnetoconductivity at $T=4.2$ K for the results of Fig. 9 for the 3.4×10^{14} cm^{-3} excess concentration.

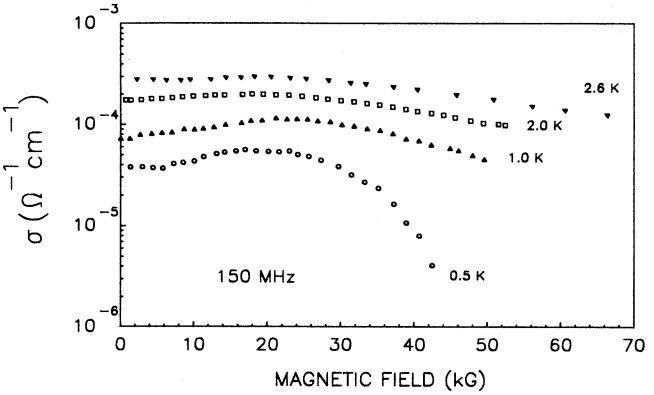

FIG. 14. ac magnetoconductivity at low temperatures for the results of Fig. 12 for the 7.5×10^{15} cm^{-3} excess concentration.

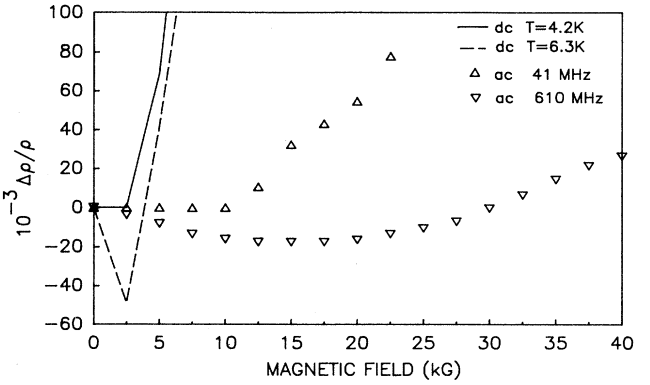

FIG. 16. Magnetoresistance data at low field for the 10^{14} cm^{-3} excess concentration. The solid curves represent dc data at $T=4.2$ K (——) and $T=6.3$ K (— — —), respectively, while ac data at $T=4.2$ K are shown at 41 and 610 MHz.

C. Magnetoresistance in the hopping regime

As we said earlier, in all our magnetoacoustic measurements (Figs. 13–15), we have seen that in some conditions a negative magnetoresistance has been observed at low field. In this section, we will discuss more thoroughly the data in Fig. 15 on the lowest concentration since for this sample, some dc resistivity data have been obtained. Consequently a full comparison between dc and ac magnetoresistance is possible.

We have gathered in Fig. 16 some of our dc data[9] at 4.2 and 6.3 K with the ac results of Fig. 15 at 41 and 610 MHz. This figure makes the emphasis on the negative magnetoresistance at low field. The dc resistivity data show that negative magnetoresistance occurs at a field below 5 kG only at some critical temperature. We observed a small ac negative magnetoresistance near 15 kG only at the highest frequency.

Negative magnetoresistance has been found in both lightly doped[15,16] and heavily doped[17] p-type InSb, as well as in degenerate semiconductors.[18] A variety of explanations[18–20] including pressure and magnetic-field-dependent activation energies, magnetic scattering centers, and tunnel hopping have been advanced but the situation seems very unclear. These works suggest that negative magnetoresistance can be obtained in a wide range of doping conditions. Unfortunately in our work we do not have sufficient data in various conditions to be able to predict a systematic field dependence. Moreover, no theory has dealt with the effect of frequency on the negative magnetoresistance. However for our ac data, it is useful to summarize our low-field results.

(1) The onset frequency at which we measured negative magnetoresistance seems to increase as we increased the acceptor concentration (Figs. 13 and 15).

(2) As the temperature is reduced, the negative magnetoresistance is more pronounced (Fig. 14).

(3) The ac negative magnetoresistance appeared at a higher magnetic field than for the dc case.

In Fig. 17 we show the same data as in Fig. 16 but for the full range of magnetic field. The most noticeable feature is the strong reduction of the magnetoresistance at field above 10 kG when the frequency is increased. Microwave data[21] above 1 GHz on a higher concentration sample showed negligible magnetoresistance therefore confirming by an independent method the trend seen in our acoustic measurements. Similar results have been obtained using standard conductivity methods at lower frequency in n-type GaAs by Chroboczek *et al.*[22] and in n-type InSb by Abboudy *et al.*[23] They have been able to

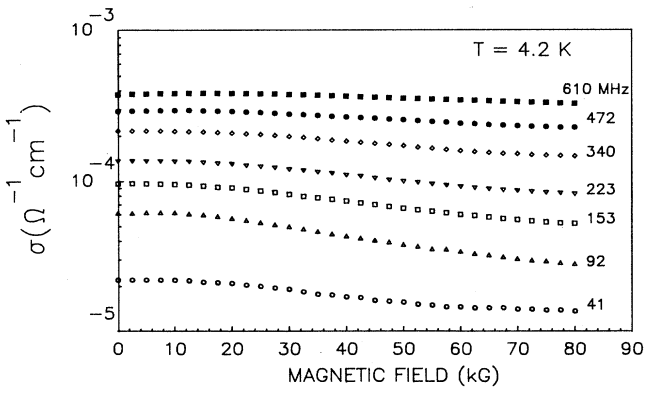

FIG. 15. ac magnetoconductivity at $T=4.2$ K for the results of Fig. 11 for the 10^{14} cm^{-3} excess concentration.

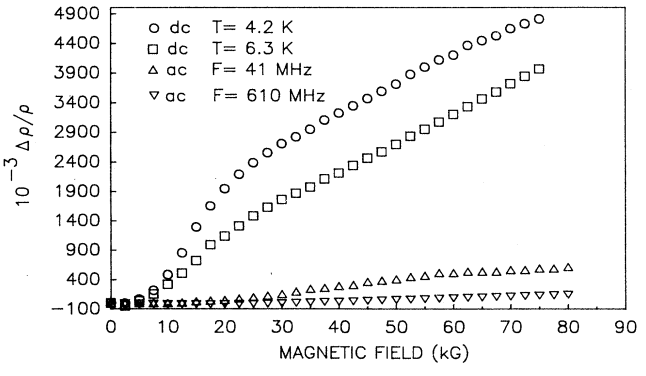

FIG. 17. Magnetoresistance data of Fig. 16 for the 10^{14} cm^{-3} excess concentration. The curves represent dc data at $T=4.2$ and 6.3 K and ac data at $T=4.2$ K for 41 and 610 MHz.

explain their magnetoresistance data in terms of the scaling theory of Summerfield[24] for disordered systems. In this theory the ac conductivity is calculated with the extended-pair approximation[25] which is a mean-field theory based upon an equivalent circuit approach for the solution of the linearized rate theory of Miller and Abrahams.[26] An empirical scaling law has been suggested for the ac conductivity in this extended-pair approximation[24]

$$\frac{\sigma(\omega)}{\sigma(0)}=F\left[\frac{A\alpha_B e^2\omega}{k_B T\sigma(0)}\right], \tag{6}$$

where α_B^{-1} is a donor Bohr radius and A is a dimensionless parameter which depends on the model used for the hopping process. It was found that experimental data on conduction in amorphous germanium, polyacetylene, and highly doped silicon were well represented by this scaling law with $F(x)=1+x^{0.725}$. To test the applicability of this model to our data, we have plotted in Fig. 18 $\log_{10}\sigma(\omega,H)/\sigma(0,H)$ versus $\log_{10}[f/\sigma(0,H)]$. This figure makes use of the ac data in Fig. 15 and of the dc data shown in Fig. 17.

It can be seen in Fig. 18 that all the data lie close to a unique curve provided $H<50$ kG since at low frequency, deviations from the universal curve increase. Furthermore our data show that a linear relationship seems to exist. If we use a more general function for $F(x)=1+x^{\beta}$, Eq. (6) can be written as

$$\log_{10}[\sigma(\omega,H)/\sigma(0,H)]=\log_{10}\{1+[f\Gamma/\sigma(0,H)]^{\beta}\}, \tag{7}$$

where $\Gamma=2\pi A\alpha_B e^2/k_B T$. If we assume that the second term on the right-hand side dominates, we can obtain an expression which satisfies a linear relationship as seen in Fig. 18,

$$\log_{10}[\sigma(\omega,H)/\sigma(0,H)]=\beta\log_{10}[f/\sigma(0,H)]+\beta\log_{10}\Gamma . \tag{8}$$

Using this equation and a straight-line fit, we find $\beta=1.0\pm0.1$ and $\Gamma=5.53\times10^{-13}$. With these numbers, it is checked that the second term in (7) dominates for $f>92$ MHz at any field $H<50$ kG. Since our measurements were made at much higher frequencies than previous works,[22–24] we cannot make an agreement with other data and we cannot say if the exponent $\beta=1.0$ that we find would decrease to the value of 0.725 suggested at lower frequency.

However our results, displayed in Fig. 18, are a clear demonstration that, in this hopping regime for a crystalline semiconductor such as p-type InSb, the frequency-dependent magnetoconductivity is suggesting that the system behaves like a disordered solid. Strong negative magnetoresistance in amorphous system such as hydrogenated amorphous silicon has been known for some time.[27] Change of sign in the magnetoresistance is suggested to be the result of the magnetic-field dependence of the spin-flip relaxation time of the charge carrier spin. Electron-spin resonance measurement gave valuable information in support of the statement that the spin density obtained in this way is closely related to the magnetoresistance effect in this compound.

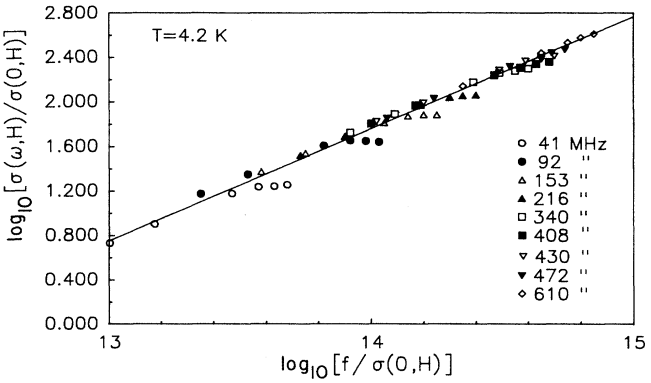

FIG. 18. Plot of the data in Fig. 17 according to Eq. (8). The solid line represents a linear fit to obtain the parameters of the scaling theory of Summerfield.

All these facts about magnetoresistance in amorphous systems and in crystalline semiconductors that we outlined previously suggest that for our results on p-type InSb a detailed study is warranted and should include dc and ac magnetoresistance data over a wide low-temperature range and magnetic field, electron-spin resonance measurements to detect localized magnetic states, and conductivity data to obtain hopping parameters. All these measurements should be done on well-characterized samples of known compensation. Finally the application of pressure should be considered since it gives complementary informations.[15–17]

V. SUMMARY AND CONCLUSIONS

This work has shown that acoustic attenuation measurements based on the piezoelectric interaction in doped semiconductors such as p-type InSb can give valuable information to study the conductivity and magnetoresistance at low temperatures.

Measurements of the zero magnetic-field attenuation as a function of temperature well below previous studies have clearly shown the difficulties in predicting a unique law to describe the ac electrical conductivity in the hopping regime. In order to make progress towards a stronger support in favor of the power law $\omega^s T^n$ for the conductivity, attenuation measurements at both higher and even lower temperature should be made during the same temperature cycling.

Magnetoresistance measurements in lightly doped p-type InSb (10^{14} cm^{-3}) have shown a negative magnetoresistance at low magnetic field in the dc and ac regimes. At high field, a strong frequency-dependent magnetoresistance was observed. For the lowest concentration a universal scaling theory used in amorphous systems was shown to give a good description of this data at $T=4.2$ K. This success is suggesting that current theories describing the negative magnetoresistance for amorphous systems might be applicable and should be considered in describing crystalline doped semiconductors in the hopping regime. However, more work is need-

ed for a full comparison with the various models.

Finally, this work on p-type InSb which has concentrated on the hopping regime has clearly established that the simple Hutson-White theory without the diffusion term is applicable and very successful in describing this semiconductor in the hopping regime.

ACKNOWLEDGMENTS

We would like to thank M. Castonguay and C. Julien for their technical support. This work was supported by Natural Sciences and Engineering Research Council of Canada (NSERC).

*Present address: Department of Physics, University of Ottawa, Ottawa, Ontario, Canada K1N 6N5.

†Present address: Department of Physics, Universidad de Los Andes, Merida 5101, Venezuela.

‡Present address: Canadian Thermostat and Control Devices, 8415 Mountain Sights, Montreal, Quebec, Canada.

[1]R. Mansfield and L. Kusztelan, J. Phys. C **11**, 4157 (1978).

[2]G. Madore and J. D. N. Cheeke, Can. J. Phys. **62**, 460 (1984).

[3]G. Quirion, M. Poirier, and J. D. N. Cheeke, J. Phys. C **20**, 917 (1987).

[4]G. Madore and J. D. N. Cheeke, Solid State Commun. **49**, 331 (1984); M. Poirier, G. Quirion, P. E. Seguin, and J. D. N. Cheeke, *ibid.* **57**, 401 (1986).

[5]E. A. Omotoso and K. A. McCarthy, J. Acoust. Soc. Am. **70**, 1707 (1981).

[6]H. Sakurai, F. Yamanaka, K. Yoshida, N. Ohshima, and K. Suzuki, J. Appl. Phys. **56**, 1613 (1984).

[7]A. R. Hutson and D. L. White, J. Appl. Phys. **33**, 40 (1962).

[8]M. Castonguay, B. Fernandez, F. Guillon, and J. D. N. Cheeke, J. Appl. Phys. **61**, 5199 (1987).

[9]G. Madore, Ph.D. thesis, University of Sherbrooke (1984).

[10]B. Fernandez, Ph.D. thesis, University of Sherbrooke (1987).

[11]F. Guillon, C. Julien, and J. D. N. Cheeke, Rev. Sci. Instrum. **58**, 1535 (1987).

[12]H. Fritzsche and K. Lark-Horovitz, Phys. Rev. **99**, 400 (1955).

[13]A. K. Walton and J. C. Dutt, J. Phys. C **10**, L29 (1977); I. N. Kurilenko, L. B. Litvak-Gorskaya, and G. E. Lugovaya, Fiz. Tekh. Poluprovodn. **13**, 1556 (1979) [Sov. Phys.—Semicond. **13**, 906 (1979)].

[14]M. Migliuolo and T. G. Castner, Phys. Rev. B **38**, 11 593 (1988).

[15]A. P. Menushenkov, E. A. Protasov, and N. A. Toloknov, Fiz. Tekh. Poluprovodn. **11**, 986 (1977) [Sov. Phys.—Semicond. **11**, 583 (1977).

[16]V. V. Galavanov and Z. A. Parimbekov, Fiz. Tekh. Poluprovodn. **13**, 120 (1979) [Sov. Phys.—Semicond. **13**, 69 (1979)].

[17]S. A. Obukhov, Fiz. Tverd. Tela (Leningrad) **19**, 1206 (1977) [Sov. Phys.—Solid State **19**, 705 (1977)]; **20**, 312 (1978) [**20**, 182 (1978)].

[18]R. P. Khosla and J. R. Fisher, Phys. Rev. B **2**, 4084 (1970).

[19]Y. Toyozawa, J. Phys. Soc. Jpn. **17**, 986 (1962); A. Kawabata, *ibid.* **49**, 628 (1980).

[20]V. L. Nguyen, B. Z. Spivak, and B. I. Shklovskii, Pisma Zh. Eksp. Teor. Fiz. **41**, 35 (1985) [JETP Lett. **41**, 42 (1985)]; Zh. Eksp. Teor. Fiz. **89**, 1770 (1985) [Sov. Phys.—JETP **62**, 1021 (1985)].

[21]M. Poirier (private communication).

[22]J. A. Chroboczek, L. Eaves, P. S. S. Guimaraes, P. C. Main, I. P. Roche, H. Mitter, J. C. Portal, P. N. Butcher, M. Ketkar, and S. Summerfield, in *Proceedings of the 17th International Conference on the Physics of Semiconductors,* edited by J. D. Chadi and W. A. Harrison (Springer-Verlag, New York, 1985), p. 697.

[23]S. Abboudy, P. Fozooni, R. Mansfield, and M. J. Lea, Philos. Mag. Lett. **57**, 277 (1988).

[24]S. Summerfield, Philos. Mag. **52**, 9 (1985).

[25]S. Summerfield and P. N. Butcher, J. Phys. C **15**, 7003 (1982).

[26]A. Miller and E. Abrahams, Phys. Rev. **120**, 745 (1960).

[27]P. Kuivalainen, J. Heleskivi, M. Leppihalme, U. Gyllenberg-Gastrin, and H. Isotalo, Phys. Rev. B **26**, 2041 (1982).